

TAILORING sp^2/sp^3 RATIO IN DIAMOND-LIKE CARBON FILMS VIA DEPOSITION PARAMETERS IN A HIGH VOLTAGE ANODIC VACUUM PLASMA

M. BADULESCU¹, A. ANGHEL¹, C. C. SURDU-BOB¹, C. LOGOFATU², C. LUCULESCU¹

¹National Institute for Lasers, Plasma and Radiation Physics, P. O. Box MG 36,
Bucharest–Magurele, 77125 Romania

E-mails: *marius.badulescu@inflpr.ro*; *alexandru.anghel@inflpr.ro*;
cristina.surdubob@inflpr.ro; *catalin.luculescu@inflpr.ro*

²National Institute for Materials Physics, P. O. Box MG. 7, Bucharest–Magurele, 77125 Romania
E-mail: *constantinlogofatu@yahoo.com*

Received May 26, 2019

Abstract. Tailoring sp^2/sp^3 ratio in diamond-like carbon thin films offers new surface engineering solutions for the continuously increasing devices requirements in various fields. We report here the control of sp^2/sp^3 carbon content using the high voltage anodic plasma in vacuum. Correlation of data obtained by visible Raman Spectroscopy and XPS spectra of our DLC films with deposition parameters showed an increase in sp^3 bonding of about 10% when decreasing the discharge voltage from 600 V to 200 V or increasing the anode-substrate distance from 15 cm to 36 cm.

Key words: diamond-like carbon thin films, Raman spectra, XPS spectra, sp^2/sp^3 ratio.

1. INTRODUCTION

Diamond-like carbon (DLC) films [1], also known as amorphous carbon films, consist of a mixture of sp^3 , sp^2 and even some sp^1 hybridized carbon bonds, with or without hydrogen content [2]. DLC is one of the most actively studied materials due to its attractive properties such as high optical transparency in the visible and infrared (IR) region, high electrical resistance, low friction coefficient, chemical inertness, high thermal conductivity and low electron affinity [3–8].

DLC films are extensively used in industry for improving surface properties of various materials and for protecting them to resist to the environment. Automotive, optics and electronics, as well as textile machinery and biomedicine are only some of the application areas of DLC films. In many of these applications one of the important information of the DLC films is sp^2/sp^3 ratio and hydrogen content which controls/understanding their properties [9].

At present, DLC films can be synthesized using a variety of plasma deposition methods such as: chemical vapor deposition (CVD) [10–12], magnetron sputtering

[13], ion plating [14], plasma laser deposition [15], mass selected ion-beam deposition [16], plasma-immersion ion implantation and deposition [17], and filtered cathodic vacuum arc deposition [18]. All these deposition methods present advantages but also drawbacks, which limit their range of applications.

A less explored deposition method for the synthesis of DLC films is the High Voltage Anodic Plasma (HVAP) known also as Thermionic Vacuum Arc plasma (TVA) [19]. Being different from other deposition methods, the expectation is to obtain DLC films with specific characteristics. Among its specific features, the following can be mentioned: the HVAP plasma does not use a buffer gas, it is localized within the deposition chamber and, also, it contains only atoms and ions of the material to be deposited. Moreover, optimization of deposition process is made by adjustment of plasma parameters [20, 21]. These characteristics allow room temperature deposition and good control of ion energy and deposition rate.

A wide range of spectroscopic techniques are used to characterize the structure and composition of DLC films. Among them, Raman spectroscopy and XPS are the most common surface techniques used in the analysis of carbon films [22, 23]. Although Raman spectroscopy does not provide quantitative information with respect to the relative amount of sp^2 and sp^3 bonding, it is an important qualitative method for evidencing the composition of DLC films. Various systematic studies and models on the variation of Raman spectra of DLC films with the sp^2/sp^3 ratio determined by complementary analysis techniques are already published [24–28].

X-ray Photoelectron Spectroscopy (XPS) is one of the standard methods used to obtain elemental composition of a surface and is often used for quantitative determination of the sp^2/sp^3 ratio in DLC films, by focusing on the C1s peak of carbon which can be deconvolved into sp^2 and sp^3 peaks [29–33].

The aim of this study was to investigate the influence of plasma process parameters (voltage and current plasma, and anode-sample distance) with sp^2 and sp^3 bonding in DLC films deposited using HVAP method and analyzed using XPS and Raman Spectroscopy.

2. EXPERIMENTAL DETAILS

Diamond Like-Carbon thin films were deposited on mirror polished single crystal (100) silicon wafers as well as borosilicate glass by HVAP. For depositing DLC, a graphite rod is used as anode. A high DC voltage (of the order of kV) is applied between the anode and a hot filament cathode. Carbon plasma of high discharge voltage (hundreds of volts) and high current (amperes) is formed above the anode. Full details of the method were described elsewhere [19, 34].

Thin DLC film growth is obtained by deposition of carbon ions and neutral atoms with fluxes depending on process parameters (discharge current I_{disc} , discharge voltage U_{disc} and anode-sample distance $D_{\text{a-s}}$). Values of the parameters used in this work are listed in Table 1. Prior to film deposition, the substrates were cleaned in ultrasonic bath with acetone and isopropyl alcohol for 15 minutes each, and were dried with nitrogen jet before loading into the vacuum chamber. The substrates were placed at 5 different distances from the electrodes on a specially designed holder. A shutter was placed between the anode and substrate holder to prevent contamination of samples prior to deposition. All depositions were conducted at room temperature in a high vacuum better than 10^{-4} Pa. After deposition, the samples were cooled down in the deposition chamber under high vacuum for at least 100 minutes.

Table 1

HVAP process parameters used for the DLC films deposition

Discharge voltage (V)	Discharge current (A)	Anode – sample distance (cm)				
200	3	15	20	23	31	36
400	2.8	15	20	23	31	36
600	2.6	15	20	23	31	36

Carbon bonding in the thin films was analyzed by Visible Raman spectroscopy. Micro Raman spectra (100 to 3200 cm^{-1}) of samples were recorded using a JASCO NRS 3100 micro-Raman spectrometer (JASCO Corporation, Tokyo, Japan), equipped with 532 nm (green) diode laser. The analyses were carried out at room temperature in ambient air.

The elemental composition was analyzed using X-ray photoelectron spectroscopy-XPS on a VG ESCA MK II system equipped with a twin anode (Mg $K\alpha$ -X ray source) with 10 eV pass energy.

3. RESULTS AND DISCUSSIONS

3.1. RAMAN SPECTROSCOPY

Raman spectroscopy is a simple and non-destructive tool that became very popular for structural characterization of carbon thin films [22–26]. The Raman spectra for visible excitation wavelength consists of two main features, the so-called G (graphite) and D (disordered) peaks centered around 1550 and 1350 cm^{-1} [35]. Although Raman spectroscopy is not able to give exact compositional information with respect to the sp^3 and sp^2 bonding of carbon atoms [36], it is commonly used as an indirect tool to probe DLC films composition qualitatively.

A typical Raman spectrum of a DLC film prepared by HVAP using the following deposition parameters: 400 V discharge voltage (U_{disc}) and 36 cm anode-sample distance ($D_{\text{a-s}}$) is shown in Fig. 1 along with the borosilicate glass substrate characteristic spectrum. The film spectrum (filled circles) consists of a broad band around 1500 cm^{-1} , which is a well-known characteristic of carbon materials attributed to the scattering of all sp^2 sites (rings and chains). The band contains a combination of G and D peaks centered on around 1560 and 1360 cm^{-1} [37–39]. A small shoulder is also observed at around 1100 cm^{-1} . This feature was attributed to scattering from the borosilicate glass substrate as evidenced by the open circles spectrum in Fig. 1.

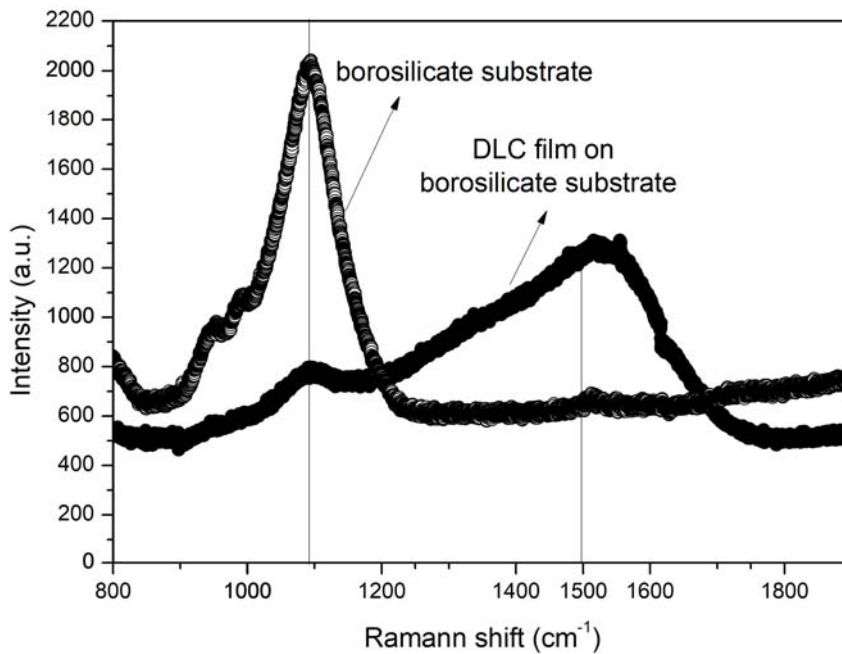


Fig. 1 – Typical Raman spectra of a DLC film prepared by HVAP using $U_{\text{disc}} = 400\text{ V}$ and $D_{\text{a-s}} = 36\text{ cm}$ (full circles) and of the borosilicate glass substrate (open circles).

Analysis of the Raman spectra for the DLC films prepared using three different deposition conditions is shown in Fig. 2. For each sample, the best theoretical fit of the raw Raman line was obtained using linear background normalization and a 90% Gaussian-Lorentzian function for both G and D peaks. Lorentz function was used for the characteristic peak of the glass substrate around 1100 cm^{-1} . The deconvoluted broad peaks corresponding to the D and G bands of graphite indicate an amorphous structure of the films [40].

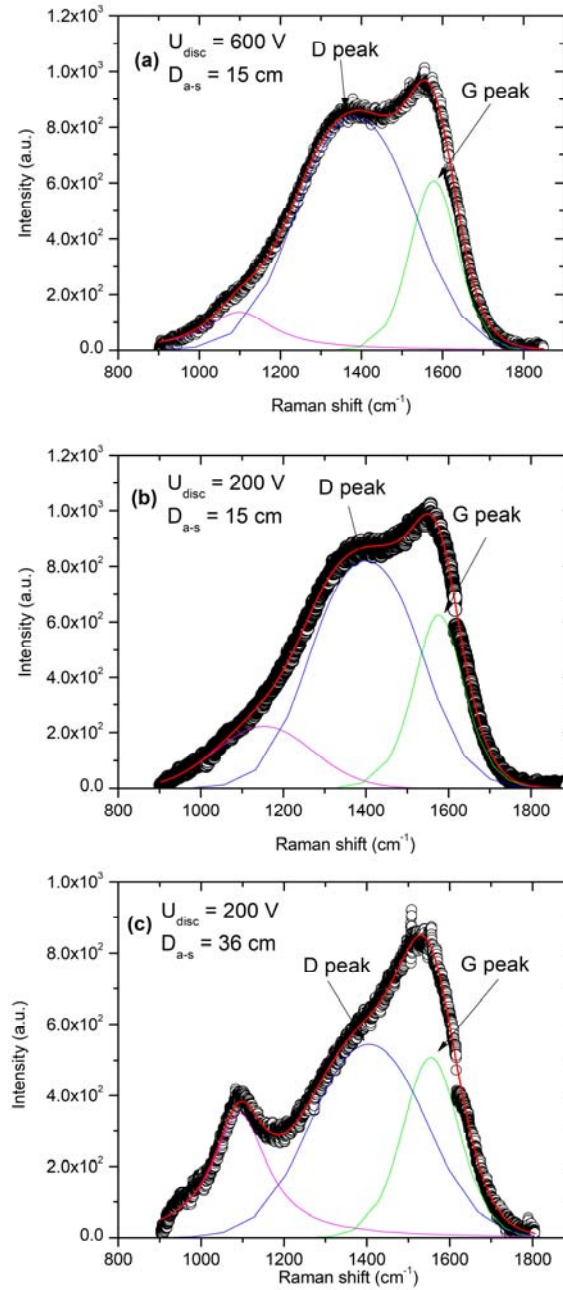


Fig. 2 – Deconvoluted Raman spectra of HVAP DLC films deposited using $U_{disc} = 600$ V and $D_{a-s} = 15$ cm (a); $U_{disc} = 200$ V and $D_{a-s} = 15$ cm (b); $U_{disc} = 200$ V and $D_{a-s} = 36$ cm (c). The solid lines correspond to a theoretical fit using a Gaussian-Lorentz cross function for both D and G peaks and a Lorentz function for the borosilicate glass substrate.

3.2. X-RAY PHOTOELECTRON SPECTROSCOPY

In order to obtain quantitative information of the sp^2/sp^3 ratio, XPS analysis is better suited [41]. Figure 3 shows a typical wide XPS spectrum of a DLC film prepared by TVA. The presence of oxygen can be observed as the only contaminant element of the film.

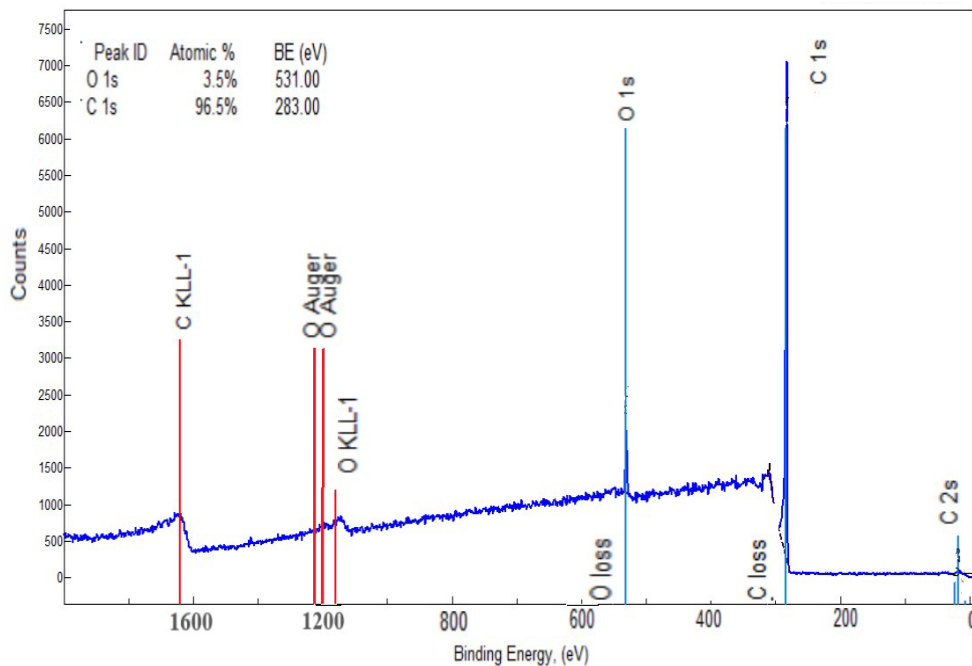


Fig. 3 – Wide XPS spectrum of a DLC film prepared by HVAP using $U_{disc} = 400$ V and $D_{a-s} = 23$ cm.

The sp^3/sp^2 fraction of carbon contained in the films was determined by deconvolution of the C 1s core level spectra. In Fig. 4 a–c, the deconvoluted C 1s band spectra corresponding to DLC films prepared by HVAP using three distinct deposition conditions are presented for comparison. The peaks centered around 285 eV and 286 eV correspond to the sp^2 and sp^3 bonding of carbon, respectively. The best fit of the C 1s level spectra was obtained by adding two more peaks most probably corresponding to an sp^2 satellite and C-O group centered at binding energy values above 286.5 eV [29, 42]. For calculation of sp^3/sp^2 fraction, the areas of these peaks were subtracted from the total C peak.

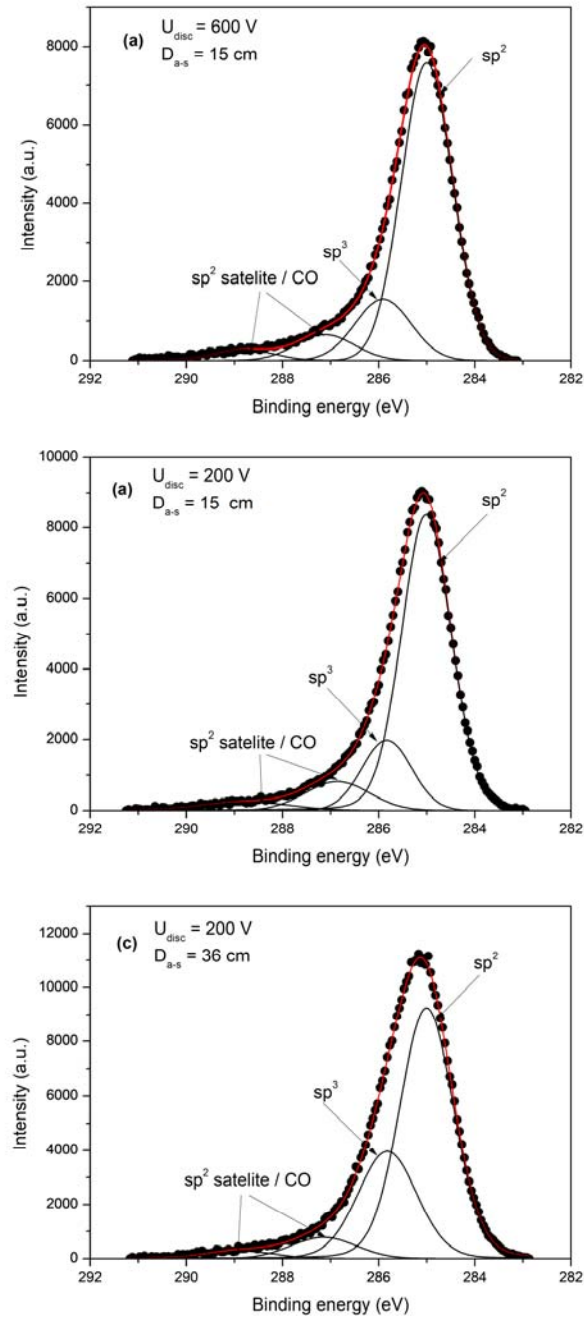


Fig. 4 – Deconvolution of C1s core level spectra Raman spectra of HVAP-DLC films deposited using $U_{disc} = 600$ V, $D_{a-s} = 15$ cm (a); $U_{disc} = 200$ V, $D_{a-s} = 15$ cm (b); $U_{disc} = 200$ V, $D_{a-s} = 36$ cm (c).

3.3. EFFECT OF THE DISCHARGE VOLTAGE ON HVAP – DLC FILMS CHARACTERISTICS

Figure 5 shows the variation of G peak position and D and G peaks intensity ratios ($I(D)/I(G)$) obtained from the deconvoluted Raman spectra as a function of the HVAP discharge voltage. An increase in the $I(D)/I(G)$ ratio with the discharge voltage from 1.11 for the film prepared at 200 V to 1.34 for the one prepared at 600 V is observed. This is attributed to the increase of the sp^2 bonded C content as well as the increase of the sp^2 clusters dimensions, as also found by other authors [27]. Additionally, the shift of the G peak position from 1554 cm^{-1} to 1563 cm^{-1} with increasing discharge voltage also indicates the increase of sp^2 content of the DLC films [43].

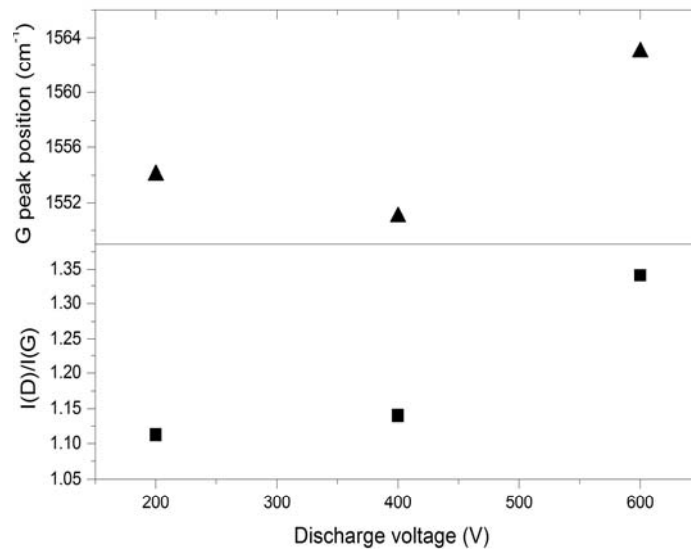


Fig. 5 – G peak position and $I(D)/I(G)$ ratio extracted from Raman spectroscopy measurements as a function of discharge voltage for the DLC films deposited at $D_{a-s} = 31\text{ cm}$.

The sp^2 and sp^3 carbon bonding fraction values, their ratios and peaks position resulted from deconvolution of XPS C 1s core level spectra of the DLC films deposited at an anode – substrate distance of 31 cm are given in Table 2 as a function of the discharge voltage. As indicated in Fig. 6, for the DLC films obtained at a distance of 31 cm from the anode the results obtained from XPS analysis revealed an increase in the sp^3 carbon bonding fraction from 19% to 29% with decreasing the discharge voltage from 600 V to 200 V. This behavior of increasing the sp^3 bonded carbon in the film by decreasing the discharge voltage was observed for all anode – substrate distances investigated in the study.

Table 2

% sp^3 and sp^2 carbon bonding fraction, their ratio and peak positions in the spectra derived from XPS analysis of DLC films prepared at $D_{a-s} = 31$ cm as a function of U_{disc}

Discharge voltage (V)	sp^3 bonded carbon (%)	sp^2 bonded carbon (%)	sp^3/sp^2 ratio	sp^3 peak position (eV)	sp^2 peak position (eV)
600	19.3	80.7	0.23	285.74	285.06
400	22	78	0.28	285.68	284.96
200	28.79	71.21	0.4	285.8	285

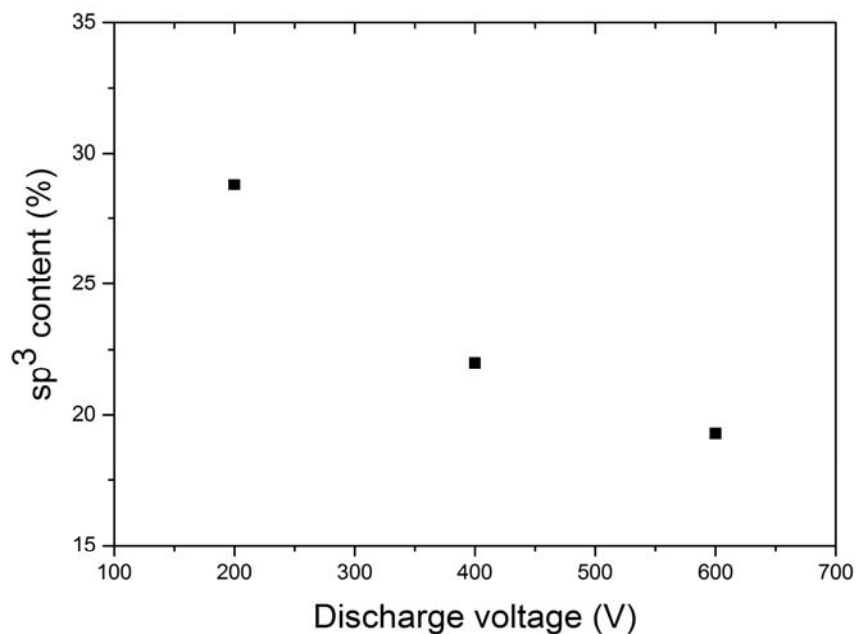


Fig. 6 – Variation of the sp^3 bonded carbon content a function of discharge voltage for the DLC films deposited at $D_{a-s} = 31$ cm.

Figure 7 shows the variation of $I(D)/I(G)$ ratio obtained from Raman analysis with sp^3 bonded carbon content obtained from XPS data. It can be observed that increasing the sp^3 content in the film leads to a decrease of the $I(D)/I(G)$ ratio. These results are in good agreement with the generally accepted interpretation of Raman spectroscopy results which correlates the increase of $I(D)/I(G)$ with a decrease of sp^3 bonded carbon content [27]. This behavior was obtained by lowering the discharge voltage of the HVAP plasma and reveals the capability of this deposition method to control DLC film composition.

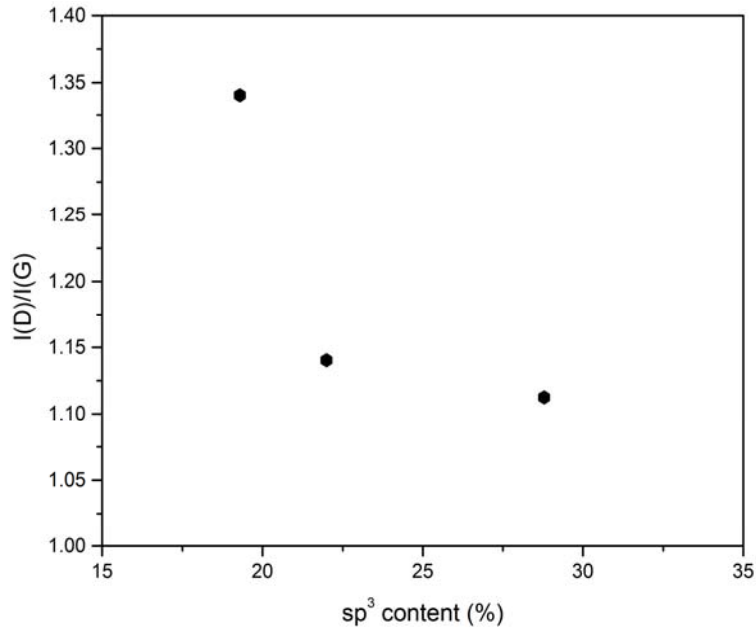


Fig. 7 – $I(D)/I(G)$ ratio as a function of sp^3 content of DLC films prepared at different discharge voltages but same anode – substrate distance ($D_{a-s} = 31$ cm).

3.4. EFFECT OF THE ANODE – SUBSTRATE DISTANCE ON HVAP – DLC FILMS CHARACTERISTICS

We observed that decreasing discharge voltage results in a higher concentration of sp^3 bonded carbon in DLC films prepared by HVAP plasma. In the following, the anode-sample distance role in tailoring the DLC films characteristics is assessed.

Figure 8 shows variation of both D and G bands ratio and G peak position with the anode – sample distance obtained from Raman spectroscopy. A monotonic decrease of the $I(D)/I(G)$ ratio is observed with increasing the anode-sample distance from 15 cm to 36 cm. Also, a shift to lower wave-number of the G peak position with increasing the anode-sample distance from 1573 cm^{-1} for the sample situated at 15 cm above the anode to 1553 cm^{-1} for the one situated at 36 cm can be observed. The decrease of $I(D)/I(G)$ ratio is attributed to the decrease of sp^2 bonded carbon content while the shift of the G peak position to lower wave-number values suggests a decrease of the sp^2 clusters size.

In Table 3, the sp^2 and sp^3 carbon bonding fraction values, their ratios and peaks position resulted from deconvolution of XPS C 1s core level spectra of the DLC films deposited by applying a 200 V discharge voltage are given as a function of the anode – substrate distance (D_{a-s}). As indicated in Fig. 6, the XPS analysis revealed that for the films obtained when 200 V discharge voltage was applied an increase in the sp^3 carbon bonding fraction from 19% to 29% with increasing the

anode-substrate distance from 15 cm to 36 cm. This behavior of increasing the sp^3 bonded carbon in the film by decreasing the discharge voltage was observed for all anode-substrate distances investigated in the study.

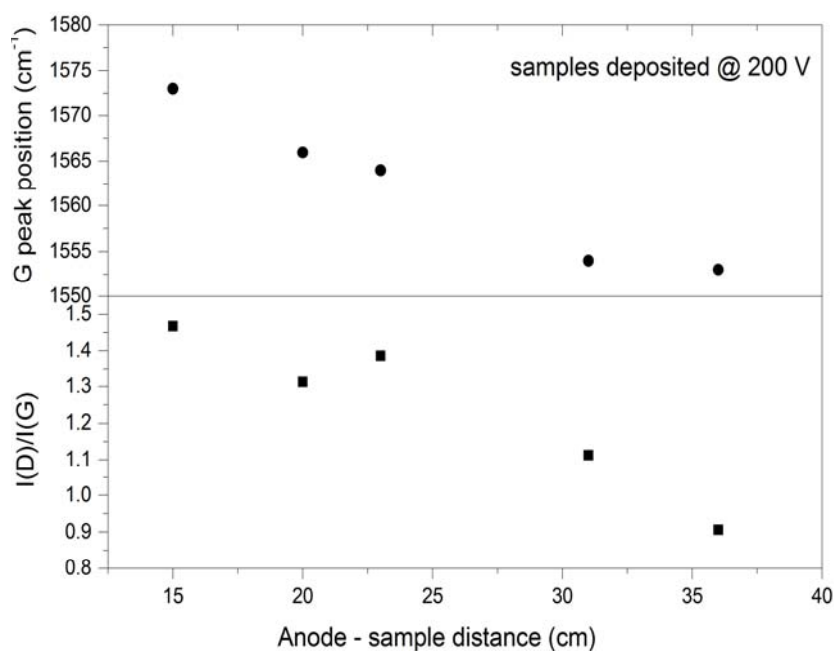


Fig. 8 – Variation of the $I(D)/I(G)$ ratio and G peak position with the anode – sample distance obtained from Raman spectroscopy for the DLC samples prepared using 200 V discharge voltage.

Table 3

% sp^3 and sp^2 carbon bonding fraction, their ratio and peak positions in the spectra derived from XPS analysis of DLC films prepared at $U_{disc} = 200$ V as a function of D_{a-s}

Anode-substrate distance (cm)	sp^3 bonded carbon (%)	sp^2 bonded carbon (%)	sp^3/sp^2 ratio	sp^3 peak position (eV)	sp^2 peak position (eV)
15	20.12	79.88	0.25	285.97	285
20	23.32	76.68	0.30	285.92	285
23	25.11	74.89	0.33	285.9	285
31	28.79	71.21	0.40	285.8	285
36	31.06	68.94	0.45	285.87	285

The XPS analysis results showed that the sp^3 content of the DLC films increased from ~ 20% to ~ 31% by increasing the anode – sample distance from 15 cm to 36 cm as evidenced in Fig. 9.

In Fig. 10 the variation of the $I(D)/I(G)$ ratio from Raman spectroscopy as a function of sp^3 content from XPS measurements is shown.

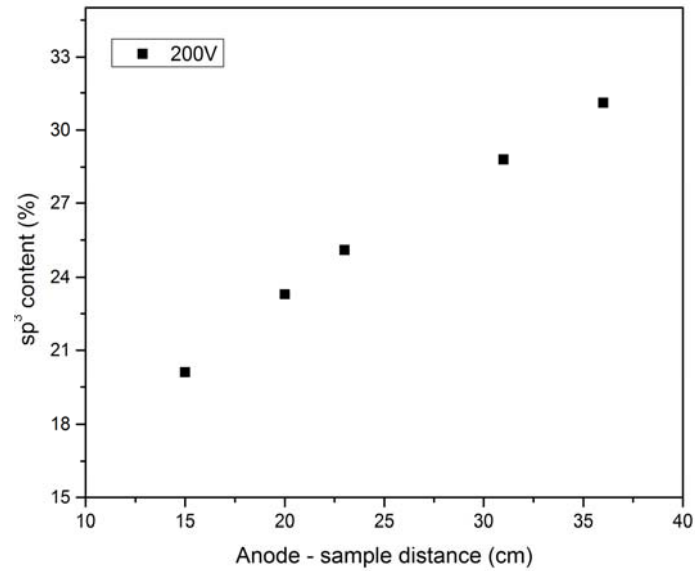


Fig. 9 – Variation of sp^3 content (in%) with anode-sample distance for DLC films prepared at a discharge voltage of 200 V.

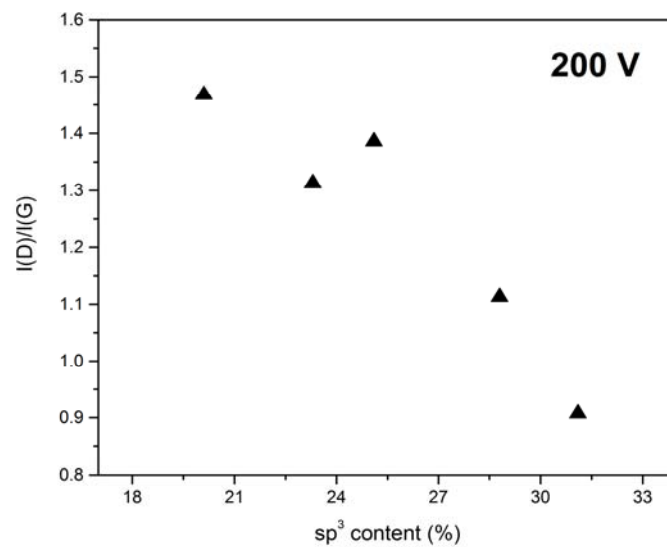


Fig. 10 – $I(D)/I(G)$ ratio vs. sp^3 content for DLC samples prepared using 200 V discharge voltage at various anode-sample distances.

As in the case of discharge voltage, the results obtained by XPS analysis are in good agreement with Raman spectroscopy. They correlate the decrease of *D* and *G* bands intensities ratio with an increase of sp³ bonded carbon atoms.

4. CONCLUSIONS

The influence of deposition parameters such as discharge voltage and anode – sample distance in HVAP plasma on the type of carbon bonding in DLC films was studied.

Visible Raman spectroscopy performed using the 532 nm excitation wavelength and also XPS analysis were used for the investigation of DLC film composition and morphology. A good agreement of our data with the generally accepted theory whereby a decrease in I(D)/I(G) ratio is accompanied by an increase of sp³ ratio was obtained.

The results obtained revealed that lowering the discharge voltage and/or increasing the anode – substrate distance results in the preferential sp³ bonding in DLC films.

The work showed that the HVAP plasma could be successfully used for tailoring DLC films according to the requirements of various applications.

Acknowledgements. This work was supported by a grant of the Romanian National Authority for Scientific Research and Innovation, CNCS-UEFISCDI, project LAPLAS VI No. 16N/8.02.2019.

REFERENCES

1. S. Aisenberg, R. Chabot, J. Appl. Phys. **42**, 2953–2958 (1971).
2. J. Robertson, Japanese Journal of Applied Physics **50**, 1S1, 01AF01-1-8 (2011).
3. K. Bewilogua, D. Hofmann, Surf. Coat. Technol. **242**, 214–225 (2014).
4. J. Robertson, Phys. Status Solidi (a), 2233–2244 (2008).
5. G. Dearnaley, J.H. Arps, Surf. Coat. Technol. **200** 2518–2524 (2005).
6. W. Song, Y. Kim, D.S. Jung, S. Il Lee, W. Jung, O.J. Kwon, H.K. Kim, M.S. Kim, K.S. An, C.Y. Park, Appl. Surf. Sci. **284**, 53–58 (2013).
7. W.S. Choi, K. Kim, J. Yi, B. Hong, Mater. Lett. **62**, 577–580 (2008).
8. C. Love, R. Cook, T. Harvey, P. Dearnley, R. Wood, Tribol. Int. **63**, 141–150 (2013).
9. C. Donnet, A. Erdemir (Eds.), *Tribology of Diamond-Like Carbon Films*, Springer, New York, 2008.
10. J. B. Wu, J. J. Chang, M. Y. Li, M. S. Leu, and A. K. Li, Thin Solid Films **516**, 2–4, 243–247 (2007).
11. L. Martinu, A. Raveh, D. Boutard, S.H. Houle, D. Poitras, N. Vella, M. Wertheiner, Diam. Relat. Mater., **2**, 5–7, 673–677 (1993).
12. L. Martinu, A. Raveh, A. Domingue, L. Bertrand, J.E. Klemberg-Sapieha, S.C. Gujarathi, M.R. Wertheiner, Thin Solid Films **208**, 1, 42–47 (1992).
13. Q. Wei, J. Sankar, J. Narayan, Surface and Coatings Technology **146–147**, 250–257 (2001).
14. J. Schwan *et al.*, J. Appl. Phys. **79**, 1416 (1996).

15. J. M Lackner, C. Stotter, W. Waldhauser, R. Ebner, W. Lenz, M. Beutl, *Surface and Coatings Technology* **174–175** 402–407 (2003).
16. Y. Lifshitz, S.R. Kashi, J.W. Rabalais, *Materials and Manufacturing Processes* **3**, 2, 157–194 (1988).
17. J. Pelletier and A. Anders, *IEEE Transactions on Plasma Science* **33**, 6, 1944–1959 (2006).
18. A. Anders, W. Fong, A.V. Kulkarni, F.W. Ryan, C.S. Bhatia, *IEEE Transactions on Plasma Science* **29**, 5, 768–775 (2001).
19. C. Surdu-Bob, I. Mustata, C. Jacob, General characteristics of the thermoionic vacuum arc plasma, *J. Opto. Adv. Mater.* **9**, 9, 2932–2934 (2007).
20. M. Badulescu, I. Gruia, C. Surdu-Bob, C. Iacob, *J. Opto. Adv. Mater – Rapid Communications* **3**, 12, 1269–1272 (2009).
21. M. Badulescu, I. Gruia, C. Surdu-Bob, C. Iacob, *J. Opto. Adv. Mater – Rapid Communications* **3**, 11, 1231–1234 (2009).
22. A. C. Ferrari and J. Robertson, *Physical Review B – Condensed Matter and Materials Physics* **61**, 20, 14095–14107 (2000).
23. P. Mérel, M. Tabbal, M. Chaker, S. Moisa, J. Margot, *Applied Surface Science* **136**, 1–2, 105–110 (1998).
24. Praver S, Nugent KW, Lifshitz Y, Lempert GD, Grossman E, Kulik J, Avigal I, Kalish R. *Diam Relat Mater.* **5**, 433–438 (1996).
25. A.V. Stanishevsky, L. Yu. Khriachtchev, *Diamond Relat. Mater.* **5**, 1355–1358 (1996).
26. L.Yu. Khriachtchev, R. Lappalainen, M. Hakovirta, M. Räsänen, *Diamond Relat. Mater.* **6**, 694–699 (1997).
27. Chen, J.P. Zhao, T. Yano, T. Ooie, M. Yoneda, J. Sakakibara, *J. Appl. Phys.* **88**, 2305–2308 (2000).
28. F.C. Tai, S.C. Lee, C.H. Wei, S.L. Tyan, *Mater. Trans.* **47**, 7, 1847–1852 (2006).
29. P. Merel, M. Tabbal, M. Chaker, S. Moisa, J. Margot, *Appl. Surf. Sci.* **136**, 1–2, 105–110 (1998).
30. J. Diaz, G. Paolicelli, S. Ferrer, F. Comin, *Phys. Rev. B* **54**, 8064 (1996).
31. A. LiBassi, A.C. Ferrari, V. Stolojan, B.K. Tanner, J. Robertson, L.M. Brown, *Diamond Relat. Mater.* **9**, 771–776 (2000).
32. A. Dorner-Reisel, L. Kubler, G. Irmer, G. Reisel, S. Schops, V. Klemm, E. Muller, *Diamond Relat. Mater.* **14**, 1073–1077(2005).
33. L. Calliari, *Diamond Relat. Mater.* **14**, 1232–1240 (2005).
34. C. Surdu-Bob, R. Vladioiu, M. Badulescu, G. Musa, *Diamond Relat. Mater.* **17**, 7–10, 1625–1628 (2008).
35. A.C. Ferrari, S. E. Rodil, J. Robertson, *Physical Review B*, **67**, 155306-1-20 (2003).
36. S. Praver, K.W. Nugent, Y. Lifshitz, G.D. Lempert, *Diamond Relat. Mater.* **5**, 433–438 (1996).
37. A.C. Ferrari, J. Robertson, *Phys. Rev. B* **64**, 7, 0754141-1-13 (2001).
38. K.W.R. Gilkes, H.S. Sands, D.N. Batchelder, J. Robertson, W.I. Milne, *Journal of Non-Crystalline Solids* **227–230**, 612–616 (1998).
39. M.G. Beghi, A.C. Ferrari, C.E. Bottani, A. Libassi, B.K. Tanner, K.B.K. Teo, J. Robertson, *Diamond Relat. Mater.* **11**, 3–6, 1062–1067 (2002).
40. W.G. Cui, Q.B. Lai, L. Zhang, F.M. Wang, *Surface and Coatings Technology* **205**, 7, 1995–1999 (2010).
41. A. Mansour, G. Indlekofer, P. Oelhafen, *Appl. Surf. Sci.* **48–49**, 312–318 (1991).
42. K. Yamamoto, Y. Koga, S. Fujiwara, F. Kokai, R.B. Heimann, *Appl Phys A*, **66**, 115 (1998).
43. B.H. Lung, M.J. Chaing, M.H. Hon, *Thin Solid Films* **392**, 1, 16–21 (2001).